Fusion Engineering and Design 190 (2023) 113652

Contents lists available at ScienceDirect

Fusion Engineering and Design

journal homepage: www.elsevier.com/locate/fusengdes

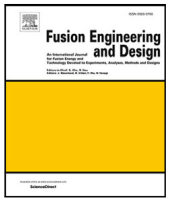

Design of an optimised movable electrostatic diagnostic for the investigation of plasma properties in a large negative ion source

Valeria Candeloro [a,b,*], Luca Calciolari [a,c], Francesco Gnesotto [a,c], Emanuele Sartori [a,c], Gianluigi Serianni [a,d], Lauro Trevisan [a], Roberto Pasqualotto [a,d]

[a] Consorzio RFX, Corso Stati Uniti 4, Padova, 35127, PD, Italy
[b] Centro Ricerche Fusione (CRF) - UNIPD, Corso Stati Uniti 4, Padova, 35127, PD, Italy
[c] Università degli Studi di Padova, Via VIII Febbraio 2, Padova, 35122, PD, Italy
[d] CNR – ISTP, Corso Stati Uniti 4, Padova, 35127, PD, Italy

ARTICLE INFO

MSC:
00A79

Keywords:
Langmuir probe
SPIDER
Negative ions

ABSTRACT

This contribution describes the design of a movable Langmuir probe system to be permanently installed in the SPIDER negative ion source. This diagnostic aims at measuring the axial profiles of plasma density, electron temperature and floating potential in both the driver and the expansion region, with a view to further investigate the positive ion dynamics. Furthermore, a deeper understanding of the plasma formation mechanism and of the RF coupling can be provided, e,g. via the estimation of the Electron Energy Distribution Function (EEDF) inside the driver. Thermal analyses were performed to define both the allowable duration of the probe exposure to the plasma and the extent of the voltage sweep. The maximum exposure time for the probe shaft is 10 s, thus a fast manipulation system is included in the design. The integration in the SPIDER source is described, considering all the limitations due to the space availability, the presence of the RF generators and the vacuum-compatibility requirements. To comply with all the constraints, several solutions are proposed for the probe head design.

1. Introduction

Negative-ion based Neutral Beam Injectors (N-NBI) are one of the envisaged heating systems for the ITER plasma. In order to comply with the heating power requirements (33 MW), a highly electronegative hydrogen/deuterium plasma is needed to extract and accelerate a precursor negative ion beam to sufficiently large beam energy. The operation of fusion-relevant negative ion sources relies on: (a) the presence of a magnetic filter field to decouple the plasma formation region, which is characterised by high plasma density and electron temperature ($n > 10^{18}$ m^{-3}, $T_e > 10$ eV), from the extraction region, where the density decreases and a much lower T_e is needed to prevent the destruction of negative ions; (b) caesium evaporation, which increases the negative ion availability (hence the beam current) via a surface production mechanism [1].

These features entail the source plasma properties along the beam axis to vary significantly from one region to another, ultimately affecting the main beam features, i.e. current density and divergence.

Several experiments [2] are currently underway to tackle all the technical and physical issues of operating giant, RF-based, caesium-assisted negative ion sources. The SPIDER [3] experiment (Source for the Production of Ions of Deuterium Extracted from a Radiofrequency plasma), hosted at Consorzio RFX in Padua, is the full-size prototype of the ITER Heating Neutral Beam (HNB) ion source equipped with a 100 kV accelerator. The effect of the source parameters on the axial plasma profiles has been characterised in SPIDER by means of a temporary set of movable electrostatic sensors [4]; this analysis though was performed in pure volume operation and without beam extraction, as the sensors entered the ion source from downstream the accelerator.

This work describes the design of a permanent movable Langmuir probe to be installed in the SPIDER source: this diagnostic will help the characterisation of the driver plasma at the resumption of the SPIDER operations, which envisages a first phase aimed at the commissioning of the new RF solid-state generators that will replace the tetrode-based oscillators in the RF circuit [5]. Subsequently, the probe head can be modified aiming at further characterising the correlation between plasma properties and operating parameters of the source, at measuring the axial profiles of positive ion density, electron temperature and floating potential with high spatial resolution, and at providing an estimate of the Electron Energy Distribution Function (EEDF) [6].

* Corresponding author at: Centro Ricerche Fusione (CRF) - UNIPD, Corso Stati Uniti 4, Padova, 35127, PD, Italy.
E-mail address: valeria.candeloro@igi.cnr.it (V. Candeloro).

https://doi.org/10.1016/j.fusengdes.2023.113652
Received 17 October 2022; Received in revised form 22 January 2023; Accepted 10 March 2023
Available online 15 March 2023

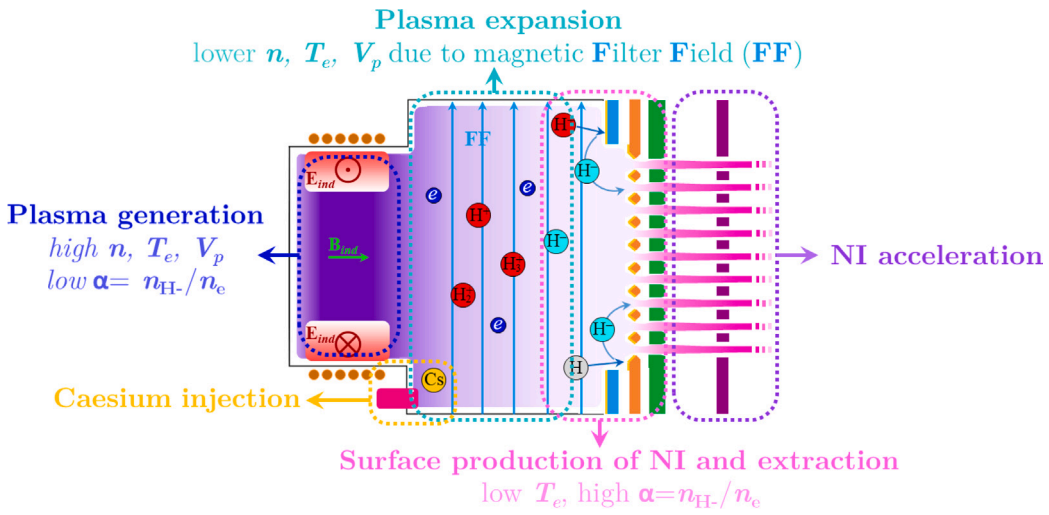

Fig. 1. Simplified scheme of a giant, caesium-assisted negative ion source. The different regions and the related plasma characteristics are highlighted.

2. Plasma–surface interaction

A Langmuir probe [7] is mainly composed of a metallic electrode electrically insulated from its support: the former collects a current $I(V)$ whose value depends on the potential difference between the probe electrode itself and the surrounding plasma, and on the plasma properties, as further explained in Appendix. The power density W on a surface exposed to the plasma will also depend on the local plasma parameters and on the surface voltage V_w as:

$$W = j_+ \left(V_w - V_P\right) + 4\pi j_e T_e + j_- T^+ \tag{1}$$

where j_+, j_e and j_- are the positive ion, electron and negative ion current densities respectively defined as:

$$j_+ = \frac{1}{4} q n_+ u_B \tag{2}$$

$$j_e = \frac{1}{4} q n_e \sqrt{\frac{8qT_e}{\pi m_e}} \exp\left(\frac{V_w - V_P}{T_e}\right) \tag{3}$$

$$j_- = \frac{1}{4} q n_- \sqrt{\frac{qT_+}{m_-}} \tag{4}$$

With the exception of the elementary charge q and the electron mass m_e, all the quantities in Eqs. (1)–(4) depend on the spatial coordinate z along the source axis. As already mentioned, Eq. (1) can be applied to any surface exposed to the plasma; however, for metallic surfaces, the surface voltage $V_w(z)$ is either equal to an externally imposed potential, or to the floating potential V_f. In the case of a non-homogeneous plasma, V_f can be obtained by imposing the floating condition (i.e. zero net collected current) on the entire surface S, thus $I_s = \int_S (j_+(z) - j_e(z) - j_-(z)) dS = 0$.

2.1. Plasma parameters

The movable Langmuir probe will measure the plasma properties in both the driver and the expansion region of the SPIDER ion source. This requires the probe stroke to cover most of the source depth, which is 40 cm. Fig. 1 shows a simplified scheme of a SPIDER-like ion source.

The expected plasma properties [8] in the driver region are $n_+ \propto 10^{18}$ m^{-3}, $T_e > 10$ eV, $V_P > 50$ V. In the expansion region, instead, the plasma density is expected to drop by a factor of 10, the electron temperature is strongly reduced ($T_e < 5$ eV) due to the presence of a magnetic filter field and, consequently, the plasma potential is also expected to decrease. It is worth pointing out that the filter field intensity in the expansion region is rather low (<5 mT), therefore plasma ions can be assumed to be not magnetised.

As caesium was injected inside the source, the plasma electronegativity (i.e. the ratio between negative ion n_- and electron n_e density) in the extraction region was found to rise up to $\alpha = 3$ close to the Bias Plate, and even further to $\alpha = 6.5$ in the proximity of the Plasma Grid apertures [9]. Fig. 2a shows the expected plasma power density flux calculated for plasma parameters measured in the SPIDER source with an injected RF power of 50 kW/driver, obtained with Eq. (8); Fig. 2b and Fig. 2c instead show theoretical CV characteristics as described by the model in the Appendix, for a single cylindrical Langmuir probe. In particular, Fig. 2b shows the CV curves for the driver plasma parameters with three different electrode diameters, whereas Fig. 2c shows CV curves expected in the expansion region for two electronegativity values.

Operating the probe in different conditions might require to apply different theories for the analysis of the Current–Voltage (CV) characteristics, which in turn can have specific validity ranges depending also on the electrode dimensions [10].

3. Probe design

3.1. Probe head design

The probe head will be composed of a tungsten (W) electrode of cylindrical shape. The electrode dimensions (both diameter and length) should be chosen while considering both physical and technical issues. First of all, the probe collecting surface affects the maximum collected current: however, for the electrodes considered in the following, the collecting surface is anyway too small to cause a significant perturbation of the surrounding plasma (as confirmed by plasma light [11] measurements performed when the previous set of movable Langmuir probes was installed in SPIDER).

Furthermore, it is known that the ratio between the electrode radius r and the Debye length λ_{De} determines which Langmuir probe theory can be used to analyse the CV characteristics, hence the accuracy of the estimation of the plasma parameters; the EEDF measurement, instead, can be performed regardless of the electrode dimension, provided that the latter is biased at least up to $V = V_P$ [10].

As for the technical issues, especially in the driver region there is a high risk of melting the probe electrode: it is therefore necessary to guarantee the endurance of the electrode to the expected thermal loads, as the probe is required to be permanently installed and routinely operated.

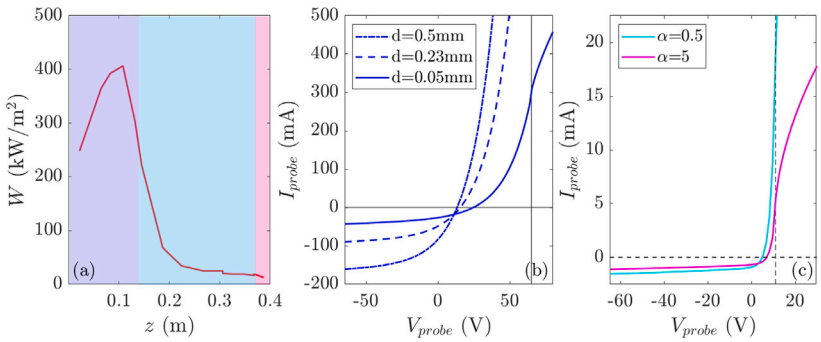

Fig. 2. (a) Expected power density for a floating object as a function of the position along the source axis; (b) simulated CV characteristic for the driver plasma with three different electrode diameters, electrode length L = 5 mm, (n = 3.5×10^{18} m^{-3}, T_e = 17 eV, V_P = 65 V); (c) simulated CV characteristic for the expansion ($\alpha = 0.5$) and extraction ($\alpha = 5$) regions, with electrode diameter 0.23 mm and length 5 mm, ($n = 2 \times 10^{17}$ m^{-3}, T_e = 2 eV, V_P = 10 V).

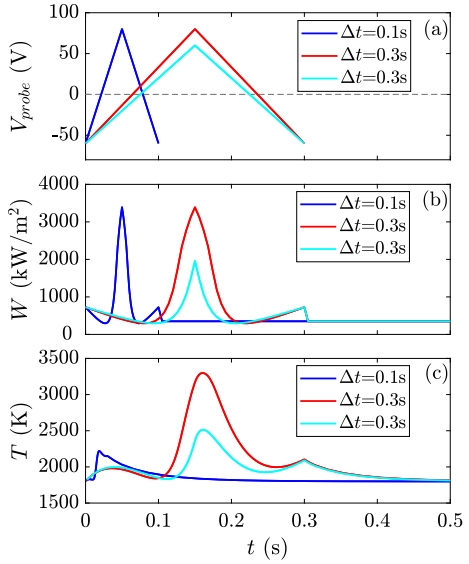

Fig. 3. Probe voltage V (a), power density W (b) and electrode temperature T (c) as a function of time for three different combinations of sweeping time Δt and maximum probe potential.

3.1.1. Thermal response of the electrode

The probe electrode will face the toughest operating conditions in the driver: for this reason, the thermal analyses of the electrode behaviour have been performed while considering the plasma properties in this region. When floating with the plasma, a tungsten electrode of length L = 5 mm reaches a temperature of 2071, 1888 and 1789 K for a diameter d of 0.05, 0.23 and 0.5 mm respectively.

However, this steady-state temperature changes when the probe is biased with respect to the plasma potential: indeed, as described by Eq. (5), the plasma power flux impinging on the electrode also depends on the probe bias.

Fig. 3 shows the probe voltage (a), the power density on the electrode (b) and the temperature reached by the electrode (c) as a function of time. It can be noticed that, besides the electrode dimensions, the temperature reached by the latter also depends on both the sweeping time Δt, defined as the time needed for a probe potential ramp, and on the range of the potential sweep. In this regard, Fig. 4 shows the maximum temperature reached by the electrode while varying both the maximum probe potential and the sweep time.

In order to keep the electrode temperature safely below the tungsten melting point (T = 3695 K), one should either perform scans with long sweeping time but reduced potential sweep, or the other way around.

3.1.2. Requirements on the acquisition system

The maximum collected current I_{probe}^{max} is directly proportional to the probe collecting surface, therefore the electrode dimensions also determine the power supply requirements. The acquisition system design is also affected by the duration of the probe potential sweep: indeed, by using a too small Δt, the sampling of the CV curve is less effective. For instance, given a 100 kS/s sampling rate and Δt = 0.01 s, the CV curve would be sampled with only 1000 points and the signal analysis would be of difficult interpretation. On the other hand, using a large sweeping time allows both to sample the curve with much higher precision and to average out the low-frequency noise components related to plasma oscillations [12], although the thermal load can become excessive for high probe voltages and too small electrode.

3.1.3. Tungsten and molybdenum sputtering

The exposed surface of the probe support can be metallised because of sputtered tungsten or molybdenum coming from the electrode itself or the source walls respectively. This can cause the probe collecting surface to change, reducing the consistency between different measurements (see Fig. 5).

Previous experience in SPIDER has shown that, by inserting thin alumina tubes at the basis of the probe electrode, sputtered tungsten cannot deposit continuously as the tubes are heated up to temperatures larger than the alumina melting point, thus they are cyclically cleaned (Fig. 6). As the alumina tubes are melted, a larger fraction of the electrode surface is exposed, so that (also in this case) the collecting area changes. However, this variation can be tracked by periodically verifying the probe response to a reference plasma discharge with identical source parameters.

3.1.4. Richardson electrons

When the probe is positively biased with respect to the plasma, the probe electrode is heated up to very high temperatures. In these conditions thermionic emission can take place. Fig. 7 shows the expected Richardson electrons available at the probe surface normalised to the positive ion saturation current for the electrode temperature values of the red profile in Fig. 3b. Child's limit for the actual emission to the plasma was not considered here; however, the results shown in Fig. 7 imply that, by operating the probe below ≈2200 K, accurate results can be obtained even without taking into account this contribution.

However, Richardson electrons are no longer negligible for temperatures higher than 2200 K, so they must be accounted for when analysing the CV characteristics. If the ramp-up phase of the probe voltage starts from a cold electrode, the thermionic emission will only take place after the probe electrode is sufficiently heated. However, as long as the $V > V_P$ condition is verified, the Richardson electrons cannot leave the electrode surface, so they can be collected by the probe for $V \leq V_P$. This will cause a hysteresis-like behaviour that might help in the estimation of this contribution, although this reasoning holds for the first measurement of the experimental session only.

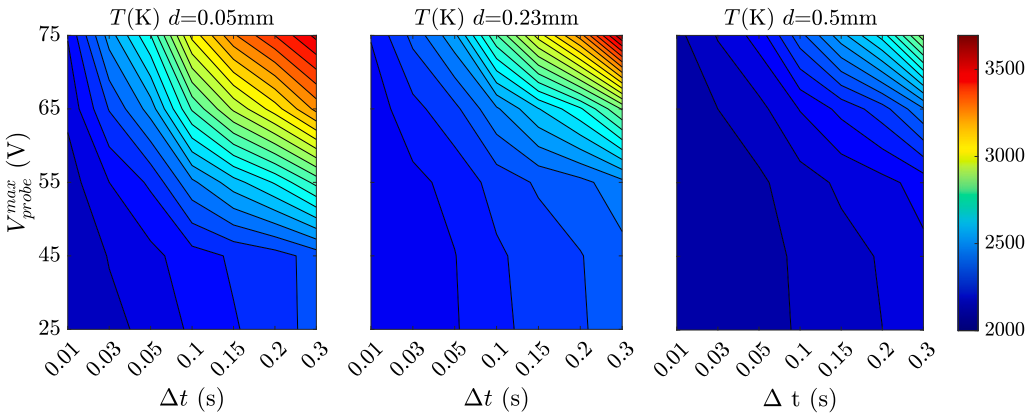

Fig. 4. Maximum temperature reached by the electrode for d = 0.05 mm, d = 0.23 mm, d = 0.5 mm as a function of the maximum probe potential V_{max} and the potential sweep time Δt.

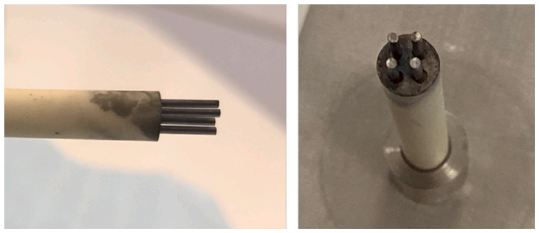

Fig. 5. Deposited W or Mo on the surface of a fixed triple Langmuir probe operated in SPIDER.

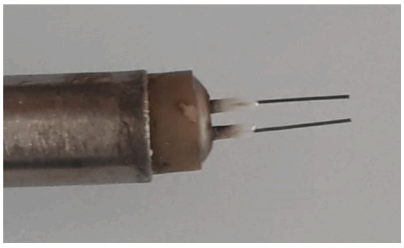

Fig. 6. Melted thin alumina tubes insulating the electrodes of a double Langmuir probe operated in SPIDER.

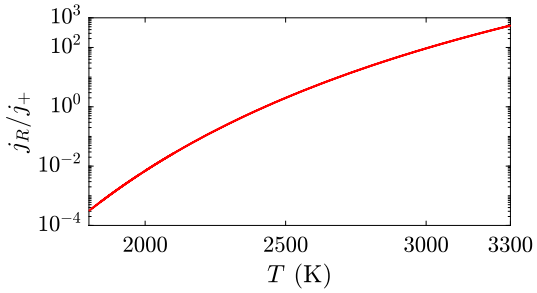

Fig. 7. Expected Richardson electron current j_R density normalised to the positive ion saturation current density as a function of the electrode temperature. The considered tungsten work function is 4.5 eV.

3.2. Probe support

The probe support consists of a bare alumina (Al_2O_3) tube or multi-bore tube either with or without a molybdenum (Mo) shielding thin tube (design 1 and 2 in Fig. 8 respectively); the presence of an external metallic surface makes the probe support structure similar to a coaxial cable, possibly shielding the RF noise, thus improving the quality of the collected signal. The multi-bore tube solution is considered with a view to design future probe heads with multiple electrodes, or even to allow the installation of a thermocouple to monitor the support temperature. Both designs have already been employed in the SPIDER ion source.

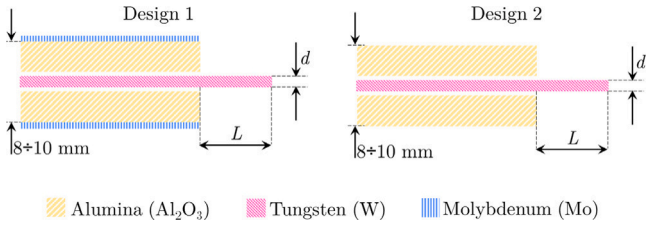

Fig. 8. Simplified schematics of two different designs for the probe support.

The probe support is required to survive inside the ion source for a sufficiently long time to perform either single or multiple measurements. According to Fig. 2a, the power density profile is not uniform along the source axis, showing a peak value of roughly 400 kW/m^2; however, in order to guarantee a safety margin, the thermal analyses of both designs were performed while considering a constant power flux profile $P(z) = P_{peak} = 450\,\mathrm{kW/m^2}$ for the entire support length, which is roughly 40 cm. Fig. 9 shows the maximum temperature reached by the (Al_2O_3) tube as a function of the exposition time, with and without the Mo shielding (design 1 and 2). The bare alumina design yields a maximum exposition time of t = 10 s, whereas in the shielded design the alumina tube resists to the thermal load for a longer time, reaching its critical temperature at t = 18 s; however, the external molybdenum rapidly heats and reaches a temperature close to its melting point: this can be an issue for the other probe components which are in contact with the support, as for instance the manipulation system (see Section 4), since the cumulated heat would be inevitably transferred.

3.2.1. RF compensation

The probe will be operated in a RF environment, therefore it is necessary to limit the RF noise via both passive and active compensation. Dealing with the former, the use of a compensation electrode [13,14] is needed especially for measuring low electron temperatures, thus mainly in the expansion and extraction regions. As explained in the following section, this Langmuir probe will be at first operated without an RF compensation electrode: indeed, the initial phase of the resumption of SPIDER operations will be mainly devoted to the characterisation of the new solid state amplifiers, therefore a simpler probe design that can be routinely operated is preferable.

Active compensation is performed by means of LC notch filters, which can be installed either:

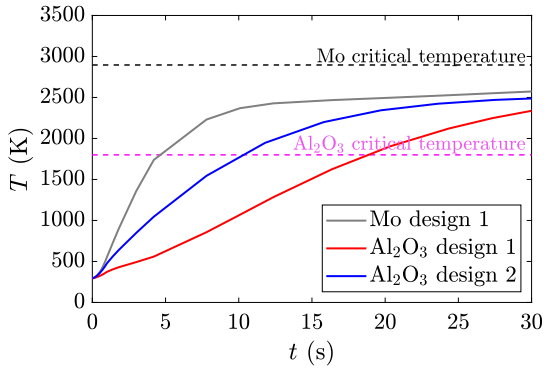

Fig. 9. Temperature reached by the alumina tube and Mo shielding as a function of time while exposed to a constant power density flux of 450 kW/m^2.

(a) as close as possible to the electrode-cable transition, in a very limited space: to this purpose, SMD-based components should be used given their reduced dimensions, although a preliminary characterisation of their behaviour at high temperatures would be mandatory;
(b) further away from the electrode-cable transition, using standard components; in this case, the filters are not necessarily mounted on the probe support and this would significantly simplify the probe head design.

3.3. Design proposals

The probe head, its support, and manipulation system are integrated in the beam source, which is biased at high negative voltages (up to −100 kV) with respect to the surrounding vacuum vessel, making the probe maintenance rather impractical; at the same time, the assessments discussed in this section imply that, at full performances of the RF driver, the expected heat load and particle flux on the probe yield quite demanding constraints for the design. For this reason, we identified a set of requirements for the probe to support the source operation, depending on the experimental phases of SPIDER:

- 1st phase: focus on the resumption of the operation with new RF circuit and drivers [15,16]. The axial density profile in the driver will be derived from the ion branch of the current–voltage characteristics; the electron temperature, expected to vary in the 10–20 eV range, will also be estimated; the dependence of the plasma properties on the source parameters will be investigated.
- 2nd phase: focus on negative ion beam optimisation. The probe will assess the role of the filter field in the optimised magnetic configuration [17]; the electron temperature is expected to decrease from 20 eV down to 1–2 eV.
- 3rd phase: focus on the plasma characterisation via movable probe together with spectroscopy: optimisation of the discharge parameters and influence of the EEDF in the driver on the negative ion precursors in the plasma and on the extracted beam current.

A single Langmuir probe that can address all the physical and technical requirements, while at the same time guaranteeing no failure and providing the required support in reaching the aims of the experimental campaigns, cannot be designed: for this reason, three different probe head types are proposed.

3.3.1. Driver probe

A robust design is proposed, with a probe head composed of an electrode with 0.5 mm diameter and 5 mm length, without RF compensation electrode, using a bare alumina tube as probe support (as design 2 in Fig. 8), with LC filters not integrated in the probe support. This probe will measure the plasma properties inside the driver while varying the source parameters, which will be extremely helpful in the early SPIDER operations devoted to the commissioning of the new RF amplifiers.

3.3.2. RF compensated probe

On the basis of the experience gained by using the aforementioned driver probe, the design will be modified to host an RF compensation electrode and to include the LC filters in the probe support, so that an accurate characterisation of the axial profiles can be performed. With SPIDER being past its first operational phase, some limitations on the source parameters (i.e. RF power/driver) can eventually be applied. Such probe could also be suitable for accurately measuring the EEDF provided that both passive and active RF compensation are integrated and that a thin electrode is used.

4. Integration in the SPIDER source

In order to integrate the probe in the SPIDER ion source [18], several aspects such as the endurance to the thermal stresses, space availability and vacuum compatibility need to be addressed. The main constraint was derived from the thermal analyses on the probe support, i.e. the maximum exposure time: the choice of the manipulation system and, consequently, the integration in the ion source have been addressed accordingly. Another important constraint is the absence of space for the integration of the actuator close to the ion source.

4.1. Choice of the actuator

The manipulation system impacts the probe measurements from different points of view: first of all, it defines the maximum probe stroke, that can be considered to be equal to the travel length of the manipulator. It also determines whether single or multiple measurements can be performed during a single exposition of the probe to the plasma, and also how many exposures the probe can endure during an experimental session. Furthermore, the source operation might be limited by the performances of the actuator, forcing operation in short plasma pulses anytime the probe is used. We can define τ_{lim} and τ_{meas} as the exposure time of the probe head and its support respectively, and τ_{mov} as the time required to position or pull-out the probe from the ion source. In this sense, the main figure of merit for the manipulator choice would be the ratio τ_{meas}/τ_{mov}, while guaranteeing that $\tau_{meas} + \tau_{mov} \leq \tau_{lim}$. Of course, a faster probe movement reduces the melting risk. In addition, the waiting time between two subsequent uses is also influenced by the choice of the actuator: the faster the manipulator, the lower the temperature of the probe components, so that the time required for the latter to cool down before the following measurement is reduced.

The SPIDER source is entirely enclosed in a vacuum vessel: for this reason, all the components of the probe – and not only the ones exposed to the plasma – are required to be vacuum-compatible. In addition, Non-Evaporable Getter (NEG) pumps will be installed during the on-going SPIDER shutdown to improve the pumping system [19]: this entails further complexity since, in order to guarantee a correct operation of the NEG pumps, all the chosen materials need to be fluorine-free and must not be affected by the high temperatures reached during the NEG regeneration.

On the basis of all these aspects, the Tecnotion® ULV linear actuator [20] was chosen as it complies with all the requirements. The basic working principle is the following: a plate equipped with coils supplied by three-phase alternating currents (called coil unit) slides along a track made of permanent magnets yokes thanks to the coupling between the magnetic field and the inductors. As the coil unit moves without friction, this system reaches relatively high speeds (up to tens of cm/s without load) and, in addition, it allows to easily pull the probe in case

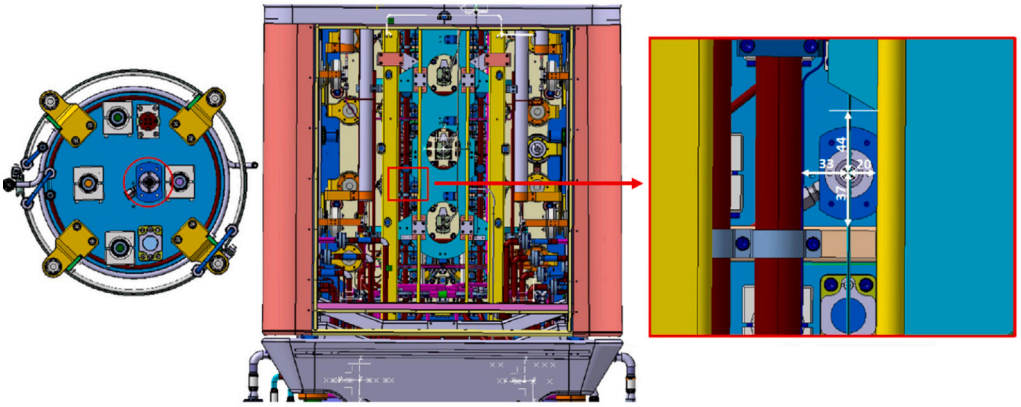

Fig. 10. Chosen probe access on the driver backplate (left), rear view of the SPIDER ion source with all its components (centre), evaluation of the distances from other source components (right). All dimensions are in mm.

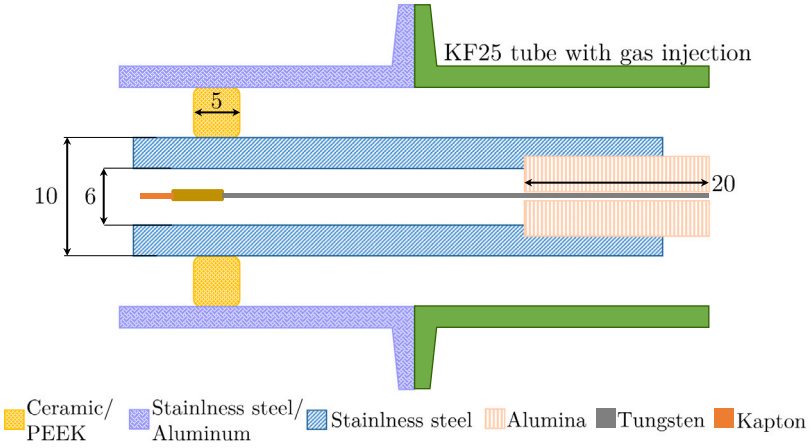

Fig. 11. Simplified scheme of the probe support-stainless steel tube transition. All dimensions are in mm.

of malfunctions. This is a unique feature, in comparison to standard axial actuators based on endless screws.

The coil unit is 259.9 mm long, whereas the length of a single permanent magnet yoke is 150 mm: by using four of the latter, the maximum available probe stroke will be (4 × 150–259.9) mm = 340 mm, that allows to cover both the driver and most of the expansion chamber.

4.2. Interface with the plasma source and sliding tube

The probe will enter the SPIDER source volume from one of the backplates of the eight RF drivers. The backplate is equipped with several ports, as shown in Fig. 10. We considered the access in the proximity of the driver centre, to allow measuring the plasma profile along the axis of the driver. This requires the probe design to guarantee vacuum holding, especially because this access is also used for gas injection. As mentioned, the actuator will be located far behind the driver backplate, due to the presence of busbars, RF lines, gas lines, diagnostics and other services of the ion source. The plasma-facing part of the probe support (either Mo-shielded or not) will be connected to a 700 mm long stainless steel tube, having an inner and outer diameter adequate to realise the transition as shown in Fig. 11, which can be secured by means of alumina-based ceramic glue.

In correspondence of this transition, the tungsten electrode will be connected to a Kapton-insulated cable that will carry the probe signal out from the ion source. For a non-shielded alumina tube, we expect a low operating temperature for the stainless steel tube as it is never exposed to the plasma, and moreover the alumina tube is sufficiently long to minimise heating by conduction.

To shield the probe from RF-induced breakdowns or contact with other elements, the former will slide inside an additional tube of either stainless steel or aluminium of approximately 600 mm length. On the source side, it will be fixed to a KF25 junction hosting the gas injection system (see also Section 4.3). As shown in Fig. 11, the two conducting tubes will be shielded from each other by means of three ceramic (or peek, which is self-lubricating in vacuum) washers: the latter have the double function of ensuring the probe alignment and of limiting the gas conductance out of the ion source. In order to guarantee the probe alignment and sliding, these washers should be thick enough (washers 5 mm thick are commercially available) and will be fixed on the moving tube. A CAD view of all these components is shown in Fig. 12.

4.3. Interface with manipulation system

The actuator is installed on a rigid support, as shown in Fig. 13. The permanent magnet yokes are fixed on an aluminium/stainless steel plate which also hosts a vacuum-compatible linear motion ball-type rolling guide. The linear guide is used to support the movable coil unit of the motor, as well as the probe shaft. This system allows the coil unit to slide at the centre of the magnet yokes. The horizontal alignment of the linear guide is essential, and will be corrected by moving the whole assembly (light blue in Fig. 13). The probe shaft will be fixed by means of two clamps, as shown in Fig. 13, allowing the refinement of the probe vertical alignment during the installation in the ion source. We estimated that with an alignment tolerance of 0.7 mrad of the linear guide, the transverse misalignment of 1 mm at the driver entrance could be easily accommodated by the rigidity of

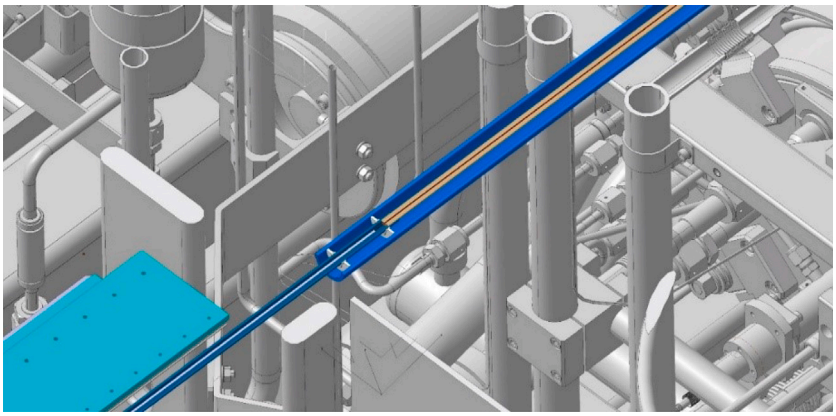

Fig. 12. CAD section of the probe: the alumina tube (probe support), inner stainless steel tube, ceramic washers and the shielding outer tube are visible.

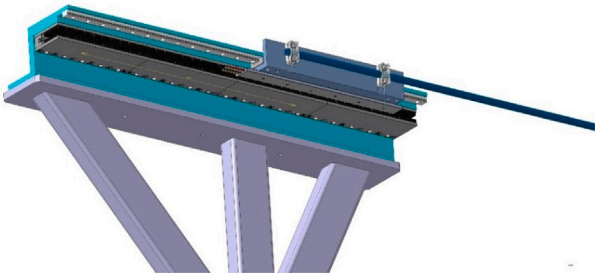

Fig. 13. Stainless steel plate hosting the permanent magnet yoke and the linear motion ball-type rolling guide.

the probe shaft assembly without opposing a significant force to the actuator movement. If larger horizontal misalignments will be detected during the installation, one of the two aforementioned clamps will be modified accordingly to allow a degree of freedom on the transverse position. The proposed design with the linear guide above the coil unit allows an easier support of a cable chain, hosting cables of the coil unit but also probe cables (not shown in Fig. 13). Finally, the coil unit will be connected to an absolute encoder in order to allow a precise determination of the probe position during the measurements. A comprehensive CAD view of the entire system integration in the SPIDER source is shown in Fig. 14 (cable chain not shown).

4.4. Integration with other diagnostics

The access chosen for the probe is shared with one of the lines of sight of the plasma light (PL), which is one of the fundamental SPIDER diagnostics [11]; indeed, the PL is a simple yet essential tool in support of the source operation as it allows a direct comparison among the eight different drivers, as long as its line of sight (LoS) is at the same relative position in all drivers (i.e. next to the driver's axis). In its current configuration, the PL telescope is installed parallel to the same access chosen for the movable probe: to preserve the PL measurement, a custom junction has been designed with an integrated mirror, with the telescope installed perpendicularly to the LoS.

Fig. 15a sketches the integration of the movable probe with the gas injection line and the PL telescope. Fig. 15b shows a section view of the junction: the left side connects to the tube integrating the gas injection system, whereas on the right side the junction supports the probe shielding tube and the manipulation structure. The openings are misaligned in such a way to leave enough room for the LoS, while mounting the telescope on the top aperture: to do so, a mirror is required (light blue element in Fig. 15) to re-direct the PL signal. This design also allows the probe to be centred with respect to the shielding tube, as in Fig. 12.

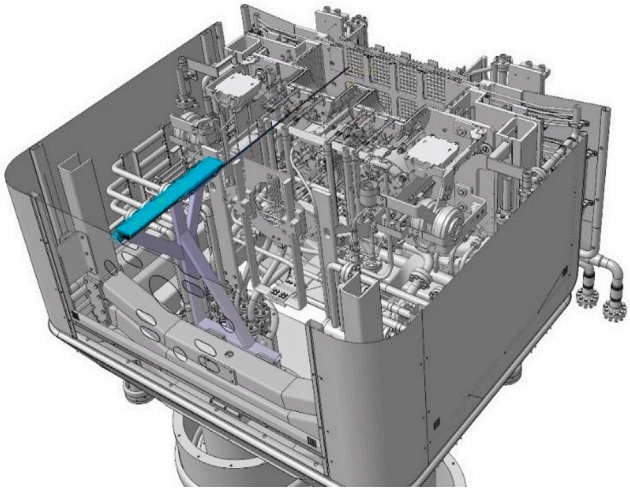

Fig. 14. CAD view of the SPIDER ion source inside the vacuum vessel with the entire probe system.

5. Conclusions

The design of a movable Langmuir probe system to be permanently installed in SPIDER is presented in this contribution. The main physical and technical aspects were discussed in order to define the main requirements of the design.

Most of the choices were based on previous experience with Langmuir probes in SPIDER, both with bare and shielded alumina supports which, owing to the limited performance of the drivers, were successfully operated without employing a fast manipulation system as the one envisaged for this project. A fast in-vacuum actuator system was designed to maximise the number of measurements, while minimising the time required for moving the probe in position. This is a key result of the design, given the short survival time of the Langmuir probe head and of its support in the high plasma density of SPIDER drivers. At full performance of 100 kW/driver, the estimated survival of the probe head is of the order of tenths of seconds, while for the probe shaft support it is of the order of tens of seconds.

The preliminary design of the system is now completed and the final design is under way, aiming at getting the system ready for installation and commissioning before the next experimental phase of SPIDER, scheduled for late 2023.

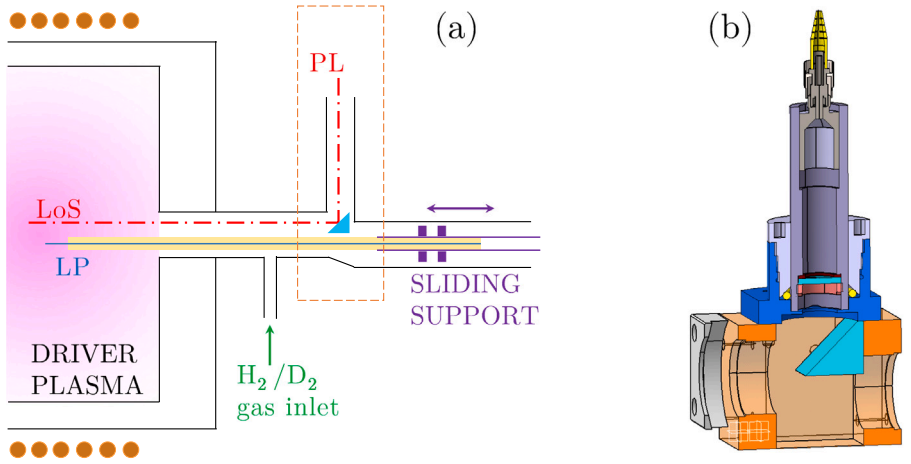

Fig. 15. (a) sketch of the integration on the axial driver port (b) custom-designed junction to hold both the probe and the plasma-light telescope.

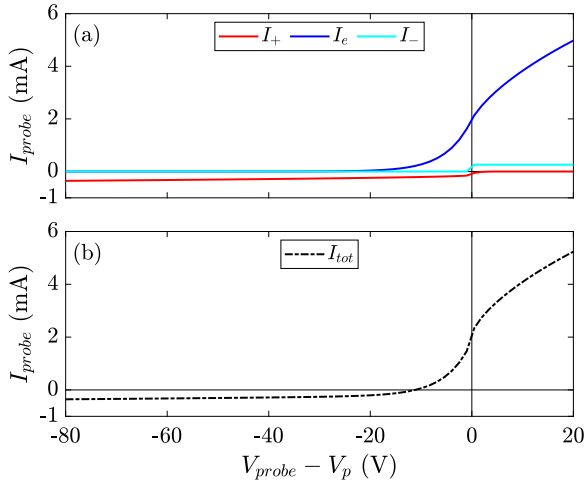

Fig. A.16. CV characteristic example for a cylindrical single Langmuir probe: (a) shows the single current contributions for positive ions I_+, electrons I_e and negative ions I_- in red, blue and cyan respectively; (b) shows the total current collected by the probe $I_{tot} = I_e + I_- - I_+$.

Declaration of competing interest

The authors declare that they have no known competing financial interests or personal relationships that could have appeared to influence the work reported in this paper.

Data availability

The authors do not have permission to share data.

Acknowledgements

This work has been carried out within the framework of the EUROfusion Consortium, funded by the European Union via the Euratom Research and Training Programme (Grant Agreement No 101052200 EUROfusion). Views and opinions expressed are however those of the author(s) only and do not necessarily reflect those of the European Union or the European Commission. Neither the European Union nor the European Commission can be held responsible for them. This work has been carried out within the framework of the ITER-RFX Neutral Beam Testing Facility (NBTF) Agreement and has received funding from the ITER Organization, France. The views and opinions expressed herein do not necessarily reflect those of the ITER Organization.

Appendix. Current collection model

Depending on the difference between the probe potential V and the plasma potential V_P, both defined with respect to the same reference potential, the probe electrode will either collect positive or negative charges. More precisely, if $V \leq V_P$, electrons close to the electrode are repelled and positive ions are collected; analogously, when $V > V_P$, negative charges will be collected. By analysing the Current–Voltage (CV) characteristics of the probe, several plasma parameters can be derived. The probe current is the sum of the positive ion, electron and negative ion contributions [21,22], labelled I_+, I_e and I_- respectively:

$$I_{tot}(V) = I_+(V) + I_e(V) + I_-(V) \tag{A.1}$$

The positive ion current reads:

$$I_+(V) = -qn_+A_{eff}(V)u_B\sqrt{\frac{1+\alpha}{1+\gamma\alpha}} \tag{A.2}$$

for $V \leq V_P$, whereas for $V > V_P$:

$$I_+(V) = -\frac{1}{4}qn_+A_g\sqrt{\frac{8qT_+}{\pi m_+}}\exp\left(-\frac{V-V_P}{T_+}\right) \tag{A.3}$$

where q is the elementary charge, n_+ is the positive ion density at sheath edge, $u_B = (qT_e/m_+)^{0.5}$ is the Bohm ion speed, $\alpha = n_-/n_e$ is the plasma electronegativity, $\gamma = T_e/T_-$ is the ratio between electron and negative ion temperature, T_+ is the positive ion temperature (in eV), m_+ is the ion effective mass, A_g is the geometrical collecting surface of the probe and A_{eff} is an effective collecting surface which accounts for the sheath expansion, thus it depends on the probe voltage. The electron current contribution can be written as:

$$I_e(V) = \frac{1}{4}qn_eA_g\sqrt{\frac{8qT_e}{\pi m_e}}\exp\left(\frac{V-V_P}{T_e}\right) \tag{A.4}$$

for $V \leq V_P$, whereas for $V > V_P$:

$$I_e(V) = \frac{1}{4}qn_eA_g\sqrt{\frac{8qT_e}{\pi m_e}}\cdot \left[2\sqrt{\frac{V-V_P}{\pi T_e}} + \exp\left(\frac{V-V_P}{T_e}\right)\mathrm{erfc}\left(\sqrt{\frac{V-V_P}{T_e}}\right)\right] \tag{A.5}$$

where n_e is the electron density at sheath edge, T_e and m_e are the electron temperature in eV and the electron mass respectively. Finally, the negative ion contribution is defined as:

$$I_-(V) = 0 \tag{A.6}$$

for $V \leq V_P$, whereas for $V > V_P$:

$$I_{-}(V) = qn_{-}A_g\sqrt{\frac{qT_{+}}{m_{-}}} \tag{A.7}$$

where n_{-} and m_{-} are the negative ion density at sheath edge and mass respectively. Fig. A.16 shows a numerical example of the current I_{probe} collected by a Langmuir probe as a function of the difference between its potential V_{probe} and the plasma potential V_P, assuming a cylindrical electrode of diameter 0.25 mm, length 5 mm.

References

[1] M. Bacal, M. Sasao, M. Wada, Negative ion sources, J. Appl. Phys. 129 (2021) 221101, http://dx.doi.org/10.1063/5.0049289.

[2] U. Fantz, et al., Ion source developments at IPP: On the road towards achieving the ITER-NBI targets and preparing concepts for DEMO, J. Phys.: Conf. Ser. 2244 (2022) 012049, http://dx.doi.org/10.1088/1742-6596/2244/1/012049.

[3] E. Sartori, et al., First operations with caesium of the negative ion source SPIDER, Nucl. Fusion 62 (2022) 086022, http://dx.doi.org/10.1088/1741-4326/ac715e.

[4] E. Sartori, et al., Development of a set of movable electrostatic probes to characterize the plasma in the ITER neutral beam negative-ion source prototype, Fus. Eng. Des. 169 (2021) 112424, http://dx.doi.org/10.1016/j.fusengdes.2021.112424.

[5] R. Casagrande, et al., Guidelines for the integration of RF solid-state generators for the high-power ion sources of NBTF experiments and ITER HNB, in: Presented at SOFT 2022.

[6] P. McNeely, S.V. Dudin, S. Christ-Koch, U. Fantz, the NNBI Team, A Langmuir probe system for high power RF-driven negative ion sources on high potential, Plasma Sources. Sci. Technol. 18 (2009) 014011, http://dx.doi.org/10.1088/0963-0252/18/1/014011.

[7] F.F. Chen, Langmuir probe analysis for high density plasmas, Phys. Plasmas 8 (2011) 3029, http://dx.doi.org/10.1063/1.1368874.

[8] V. Toigo, et al., On the road to ITER NBIs: SPIDER improvement after first operation and MITICA construction progress, Fus. Eng. Des. 168 (2021) 112622, http://dx.doi.org/10.1016/j.fusengdes.2021.112622.

[9] G. Serianni, E. Sartori, et al., Spatially resolved diagnostics for optimization of large ion beam sources, Rev. Sci. Instrum. 93 (2022) 081101, http://dx.doi.org/10.1063/5.0084797.

[10] I.D. Sudit, R.C. Woods, A study of the accuracy of various Langmuir probe theories, J. Appl. Phys. 76 (1994) 4488, http://dx.doi.org/10.1063/1.357280.

[11] R. Pasqualotto, et al., Plasma light detection in the SPIDER beam source, Fus. Eng. Des. 146 (2019) 709–713, http://dx.doi.org/10.1016/j.fusengdes.2019.01.061.

[12] V. Candeloro, G. Serianni, M. Fadone, B. Laterza, E. Sartori, Development of a triple Langmuir probe for plasma characterization in SPIDER, IEEE Trans. Plasma Sci. 146 (2022) 3871–3876, http://dx.doi.org/10.1109/TPS.2022.3173885.

[13] M.A. Lieberman, A.J. Lichtenberg, Principles of plasma discharges and materials processing, 2005.

[14] I.D. Sudit, F.F. Chen, RF compensated probes for high-density discharges, Plasma Sources. Sci. Technol. 3 (1994) 162, http://dx.doi.org/10.1088/0963-0252/3/2/006.

[15] M. Recchia, et al., Improvement in the electrical design of the SPIDER beam source, presented at SOFT, 2022.

[16] A. Maistrello, et al., Overview on electrical issues faced during the SPIDER experimental campaigns, presented at SOFT, 2022.

[17] N. Marconato, et al., Integration of new sets of magnets for improved plasma confinement in the SPIDER experiment, presented at SOFT, 2022.

[18] D. Marcuzzi, et al., Detail design of the beam source for the SPIDER experiment, Fus. Eng. Des. 85 (2010) 1792–1797, http://dx.doi.org/10.1016/j.fusengdes.2010.05.039.

[19] M. Siragusa, E. Sartori, M. Mura, F. Siviero, Numerical simulation of experimental tests performed on ZAO non-evaporable-getter pump designed for neutral beam injector applications, Rev. Sci. Instrum. 91 (2020) 023501, http://dx.doi.org/10.1063/1.5128662.

[20] Tecnotion. https://www.tecnotion.com.

[21] E. Sartori, V. Candeloro, G. Serianni, Analysis of current–voltage characteristics for Langmuir probes immersed in an ion beam, Rev. Sci. Instrum. 91 (2020) 023504, http://dx.doi.org/10.1063/1.5128669.

[22] N. Hershkowitz, How Langmuir probes work, in: Plasma Diagnostics: Discharge Parameters and Chemistry, Vol. 1, 2013.